Decoding a Neurofeedback-Modulated Cognitive Arousal State to Investigate Performance Regulation by the Yerkes-Dodson Law

Saman Khazaei, *Student Member, IEEE,* Md. Rafiul Amin *Student Member, IEEE*, and Rose T. Faghih, *Member, IEEE*

***Abstract*— Enhancing the productivity of humans by regulating arousal during cognitive tasks is a challenging topic in psychology that has a great potential to transform workplaces for increased productivity and educational systems for enhanced performance. In this study, we assess the feasibility of using the Yerkes–Dodson law from psychology to improve performance during a working memory experiment. We employ a Bayesian filtering approach to track cognitive arousal and performance. In particular, by utilizing skin conductance signal recorded during a working memory experiment in the presence of music, we decode a cognitive arousal state. This is done by considering the rate of neural impulse occurrences and their amplitudes as observations for the arousal model. Similarly, we decode a performance state using the number of correct and incorrect responses, and the reaction time as binary and continuous behavioral observations, respectively. We estimate the arousal and performance states within an expectation-maximization framework. Thereafter, we design an arousal-performance model on the basis of the Yerkes–Dodson law and estimate the model parameters via regression analysis. In this experiment musical neurofeedback was used to modulate cognitive arousal. Our investigations indicate that music can be used as a mode of actuation to influence arousal and enhance the cognitive performance during working memory tasks. Our findings can have a significant impact on designing future smart workplaces and online educational systems.**

I. Introduction

Human psychological activity is a complicated and broad topic that receives considerable attention from scholars. One of the psychological features of our brain that takes a leading role in our emotional status is called arousal [1]. Arousal can describe the state of being conscious, the degree of concentration during a specific process, and various levels of stress [1]. Thus, it can directly influence our daily routines, and maintaining a proper level of arousal may result in being productive throughout psychological and physiological activities. Therefore, regular monitoring and regulating arousal is a critical topic of study. There are several ways to monitor the arousal states of the brain during an activity. One of the most popular and non-invasive ways to evaluate the arousal state is using the electrodermal activity (EDA). The autonomic nervous system (ANS) activation is responsible for the variations in the skin conductance (a measure of EDA) via sweat secretion as an indicator of psychological arousal [2].

The other crucial attribute in studying the brain is human performance during a cognitive task, which can be affected by several psychological factors such as emotional well-being, amount of stress, and dedicated concentration. Working memory is a system in the brain that retains sensory perceptions for processing and understanding a cognitive task. Working memory is integral for day-to-day cognitive functions. The n-back task is a working memory experiment that was first introduced by Kirchner [3]. It is a common cognitive experiment that is used for evaluating working memory. In the n-back task, the participant is presented with a series of stimuli displayed one at a time, and the participant has to identify if the current stimulus is the same as the n^{th} previous one [4]. As is evident, the difficulty level increases with n, since the participant has to recall more of the stimuli with larger values of n. Lehmann et al. [5] showed that the tasks with a higher load on working memory are influenced by music. Many other studies have also recognized the ability of music to impact performance during working memory tasks [6], [7]. There is a need for investigating how different background music (e.g. calming, vexing) can influence working memory for developing a regulation strategy for enhancing performance during the tasks demanding a higher load on working memory.

The state-space methods have been widely popular in behavioral learning [8]–[12] and movement decoding in brain-computer interfaces [13], [14]. Furthermore, state-space approaches are also used to estimate arousal states from different physiological binary and continuous observations similar to [15]–[23]. However, state-space approaches have not been explored for evaluating individual performance during working memory tasks to investigate how the decoded performance varies as a function of the decoded arousal state. Therefore, we formulate a state-space approach for estimating performance state and compare it with the arousal states to investigate the feasibility of improving performance by using the Yerkes–Dodson law.

The Yerkes–Dodson law explains that throughout an activity, at a low arousal level, the performance is lower and has a positive slope while plotted against arousal level [24], [25]. At a higher level of arousal, the performance decreases with an increase in arousal. The performance stays maximum near the moderate range of arousal. Thus, the inverted-U law can be considered as a link between arousal and

This work was supported in part by by the U.S. National Science Foundation under Grants 1942585 – CAREER: MINDWATCH: Multimodal Intelligent Noninvasive brain state Decoder for Wearable AdapTive Closed-loop arcHitectures and 1755780 – CRII: CPS: Wearable-Machine Interface Architecture. This article was presented in part at the proceedings of the IEEE Engineering in Medicine and Biology Society Conference [1].

S. Khazaei, M. R. Amin, D. S. Wickramasuriya, and R. T. Faghih are with the Department of Electrical and Computer Engineering at the University of Houston, Houston, TX 77004 USA (correspondence e-mail: rtfaghih@uh.edu). Rose T. Faghih served as the senior author.

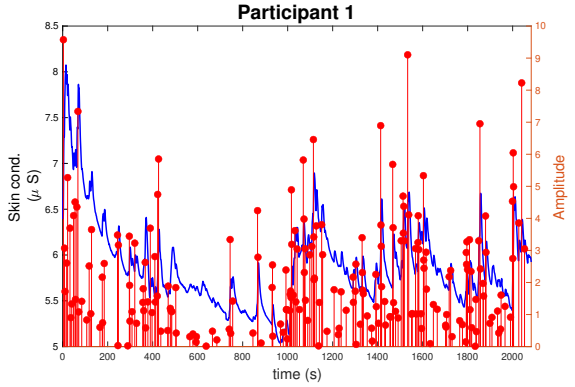

Fig. 1: **An example skin Conductance deconvolution result.** The blue curve corresponds to the raw skin conductance and red vertical line corresponds to inferred neural stimuli due to ANS activation.

performance during a cognitive task. As music can modulate individual arousal and performance [26], analyzing whether the inverted-U law also holds for a working memory task while listening to music motivated this study.

In particular, in this study, we investigate the impacts of music on performance during two n-back tasks (1-back and 3-back tasks). During this n-back experiment, the subject listened to two different kinds of background music, i.e. calming and vexing music. We collect user responses as the correct/incorrect responses and the corresponding reaction times. We also measured the skin conductance throughout the experiment. We utilize two state-space models for decoding both performance and arousal states to relate them to the corresponding observations, i.e., user behavioral responses and the skin conductance measurements, respectively. We utilize an expectation-maximization framework to estimate both the model parameters and the hidden states from the corresponding observations. Finally, we investigate the relationship between the estimated arousal and performance states.

II. Methods

A. Dataset

The experiment conducted in this research was approved by the Institutional Review Board at the University of Houston, Houston, Texas, USA. There were 6 participants and the dataset was collected by performing equivalent numbers of 1-back and 3-back task blocks with two sessions of calming and vexing background music. Each task block started with a 5 seconds instruction about the task, followed by 22 trials, with 0.5 seconds for displaying the number and 1.5 seconds for the participant to respond to the given stimulus resulting in a total of 49 seconds of total stimulus time. At the end of each trial, a 10 second RELAX section was contrived. After 8 trials (halfway mark for each session), a 20 second RELAX segment was presented and between the sessions, there was a 2-minute relaxation break where the participant was allowed to provide a response. A detailed description of the experiment is provided in [27].

B. Inference of brain activation from skin conductance Measurements

The measured skin conductance during the experiment can be thought of as a summation of two components: (1) a slow varying tonic component and (2) a fast varying phasic component [2], [28]. The tonic component is related to the body's thermoregulation and general arousal. The phasic component is defined as the convolution between the neural impulse train due to ANS activation and the physiological system response [2], [28]. For inferring the neural impulse train due to ANS activation from the raw skin conductance, we need to perform proper deconvolution. First, we pre-process the data similar to [22], [29]. Secondly, we low-pass filter the data at 0.5 Hz. Then, we remove the tonic component using cvxEDA [30]. Finally, we deconvolve the extracted phasic component to estimate the sparse ANS activation. Using a coordinate descent approach, we perform a signal deconvolution identical to [22]. Thus, we obtain sparse ANS activations (Fig. 1).

C. Arousal state-space model

Similar to [16], we define a first-order autoregressive (AR) model for a hidden cognitive arousal state x_j such that

$$x_j = x_{j-1} + \epsilon_j, \tag{1}$$

where $\epsilon_j \sim \mathcal{N}(0, \sigma_\epsilon^2)$ is the process noise and j represents the time index. Pursuing the established marked point process filtering approach for arousal state in [16], we take the occurrence of a neural impulse n_j, as a Bernoulli-distributed random variable with probability mass function $a_j^{n_j}(1-a_j)^{1-n_j}$ and $P(n_j = 1) = a_j$. We may relate x_j to a_j using sigmoid transform according to [8], and the final equation is

$$a_j = \frac{1}{1 + e^{-(x_j+\beta)}}, \tag{2}$$

where β is a constant that can be determined by $\beta \approx \log\left(\frac{a_0}{1-a_0}\right)$ and a_0 is the average probability of observing an impulse during the experiment. Similar to [16], we model the continuous-valued amplitude r_j of each neural impulse as

$$r_j = \gamma_0 + \gamma_1 x_j + v_j, \tag{3}$$

where r_j is the amplitude of the observed neural impulse due to ANS activation, $v_j \sim \mathcal{N}(0, \sigma_v^2)$ is representing the sensor noise, γ_0 and γ_1 are the unknown parameters to be determined. As a result, the joint density function for the observed neural stimuli is

$$p(n_j \cap r_j | x_j) = \begin{cases} 1 - a_j & \text{if } n_j = 0 \\ a_j \frac{1}{\sqrt{2\pi\sigma_v^2}} e^{\frac{-(r_j - \gamma_0 - \gamma_1 x_j)^2}{2\sigma_v^2}} & \text{if } n_j = 1 \end{cases}. \tag{4}$$

Utilizing an expectation-maximization framework, we are able to estimate the unknown parameters $\theta_A = \{\sigma_\epsilon^2, \gamma_0, \gamma_1, \sigma_v^2\}$, and hidden state x_j, simultaneously. Here, the E-step equations have been derived based

on the observations $R^J = \{(n_1, r_1), ..., (n_J, r_J)\}$ up to time J. At the E-step, we apply Bayesian filtering to estimate x_j and the forward filter equations are shown below.

Predict:

$$x_{j|j-1} = x_{j-1|j-1}, \tag{5}$$
$$\sigma^2_{j|j-1} = \sigma^2_{j-1|j-1} + \sigma^2_\epsilon, \tag{6}$$

Update:

if $n_j = 0$

$$x_{j|j} = x_{j|j-1} + \sigma^2_{j|j-1}(n_j - a_{j|j}), \tag{7}$$
$$\sigma^2_{j|j} = \left[\frac{1}{\sigma^2_{j|j-1}} + a_{j|j}(1 - a_{j|j})\right]^{-1}, \tag{8}$$

if $n_j = 1$

$$C_j = \frac{\sigma^2_{j|j-1}}{\gamma_1^2 \sigma^2_{j|j-1} + \sigma^2_v}, \tag{9}$$
$$x_{j|j} = x_{j|j-1} + C_j \Big[\sigma^2_v(n_j - a_{j|j}) + \gamma_1(r_j - \gamma_0 - \gamma_1 x_{j|j-1})\Big], \tag{10}$$
$$\sigma^2_{j|j} = \left[\frac{1}{\sigma^2_{j|j-1}} + a_{j|j}(1 - a_{j|j}) + \frac{\gamma_1^2}{\sigma^2_v}\right]^{-1}. \tag{11}$$

Note that $x_{j|j}$ appears on both sides of (7) and (10) and we can solve for x_j numerically by utilizing the Newton-Raphson method.

After coming to $j = J$, we reverse the direction and improve x_j by obtaining a set of smoothed mean and variance estimates. The equations for the backward smoother are

$$A_j = \frac{\sigma^2_{j|j}}{\sigma^2_{j+1|j}}, \tag{12}$$
$$x_{j|J} = x_{j|j} + A_j(x_{j+1|J} - x_{j+1|j}), \tag{13}$$
$$\sigma^2_{j|J} = \sigma^2_{j|j} + A_j^2(\sigma^2_{j+1|J} - \sigma^2_{j+1|j}). \tag{14}$$

At the M-step, we take $\tilde{J} = \{j | n_j = 1\}$ to indicate the locations where neural impulses occur. Similar to [16] and [8], we calculate the expected values of x_j^2, and $x_j x_{j-1}$ using the following,

$$\mathbb{E}[x_j^2] = x^2_{j|J} + \sigma^2_{j|J}, \tag{15}$$
$$\mathbb{E}[x_{j+1} x_j] = x_{j+1|J} x_{j|J} + A_j \sigma^2_{j+1|J}. \tag{16}$$

Using the E-step results, we obtain the log-likelihood function Q_1, we find the unknown parameters such that they maximize it. The Q_1 function is as follows,

$$Q_1 = \sum_{j=1}^{J} \mathbb{E}[n_j(\beta + x_j) - \log(1 + e^{\beta + x_j})] \tag{17}$$
$$+ \frac{-\tilde{J}}{2}\log(2\pi\sigma_v^2) - \sum_{j \in \tilde{J}} \frac{\mathbb{E}\Big[(r_j - \gamma_0 - \gamma_1 x_j)^2\Big]}{2\sigma_v^2}$$
$$+ \frac{-J}{2}\log(2\pi\sigma_\epsilon^2) - \sum_{j=1}^{J} \frac{\mathbb{E}\Big[(x_j - x_{j-1})^2\Big]}{2\sigma_\epsilon^2}.$$

The algorithm iterates between the E-step and the M-step until convergence.

D. Performance state-space model

Inspired by the state-space model in [12] for decoding a cognitive learning state, we represent the cognitive performance state as

$$z_k = \rho z_{k-1} + w_k, \tag{18}$$

where z_k is an latent performance state, $v_k \sim \mathcal{N}(0, \sigma_w^2)$ stands for process noise, ρ is the unknown coefficient; k is the trial number during the experiment.

Considering one binary observation (correct/incorrect response at k^{th} trial) and one continuous observation (reaction time of the corresponding response), similar to [12], the observation equation in terms of reaction time would be

$$I_k = \log t_k = \alpha_0 + \alpha_1 z_k + \delta_k, \tag{19}$$

where $\delta_k \sim \mathcal{N}(0, \sigma_\delta^2)$, t_k is the reaction time at each trial; we take the log of the reaction time to ensure at each trial, the reaction time estimate is positive. α_0 and α_1 are the unknown parameters.

Similar to [12], the binary response has been assumed to have a Bernoulli probability model with the probability mass function $p_k^{m_k}(1 - p_k)^{1 - m_k}$ and $P(m_k = 1) = p_k$. We relate the performance state to the probability of having correct response by applying the same sigmoid transform here and therefore,

$$p_k = \frac{1}{1 + e^{-(z_k + \mu)}}, \tag{20}$$

and similar to parameter β, the constant term μ, can be found by $\mu \approx \log\left(\frac{p_0}{1 - p_0}\right)$ where p_0 is the average probability of the correct response which is equal to $p_0 = 0.5$.

Again, the unknown parameters of the performance state model $\theta_P = \{\rho, \sigma_w^2, \alpha_0, \alpha_1, \sigma_\delta^2\}$, and the performance state z_k, can be estimated through EM approach. The E-step equation would be different from the arousal state case since we have one binary and one continuous observation at trial k. The forward filter equations in E-step are,

Predict:

$$z_{k|k-1} = \rho z_{k-1|k-1} \tag{21}$$
$$s^2_{k|k-1} = \rho^2 s^2_{k-1|k-1} + \sigma_w^2$$

Update:

$$z_{k|k} = z_{k|k-1} + \frac{s^2_{k|k-1}}{\alpha_1^2 s^2_{k|k-1} + \sigma_\delta^2}\Big[\sigma_\delta^2(m_k - p_{k|k}) \tag{22}$$

$$+ \alpha_1(I_k - \alpha_0 - \alpha_1 z_{k|k-1})\Big]$$

$$s^2_{k|k} = \left[\frac{1}{s^2_{k|k-1}} + p_{k|k}(1-p_{k|k}) + \frac{\alpha_1^2}{\sigma_\delta^2}\right]^{-1} \tag{23}$$

By reversing the direction, we may build the smoother similar to the arousal state-space model. The smoother states are as follows,

$$B_k = \rho \frac{s^2_{k|k}}{s^2_{k+1|k}}, \tag{24}$$

$$z_{k|K} = z_{k|k} + B_k(z_{k+1|K} - z_{k+1|k}), \tag{25}$$

$$s^2_{k|K} = s^2_{k|k} + B_k^2(s^2_{k+1|K} - s^2_{k+1|k}). \tag{26}$$

The expected values of z_k^2, and $z_k z_{k-1}$ are as follows,

$$\mathbb{E}[z_k^2] = z^2_{k|K} + s^2_{k|K}, \tag{27}$$

$$\mathbb{E}[z_{k+1} z_k] = z_{k+1|K} z_{k|K} + B_k s^2_{k+1|K}. \tag{28}$$

For the corresponding M-step, the expected log-likelihood function is as follows,

$$Q_2 = \sum_{k=1}^{K} \mathbb{E}[m_k(\mu + z_k) - \log(1 + e^{\mu + z_k})] \tag{29}$$

$$+ \frac{-K}{2}\log(2\pi\sigma_\delta^2) - \sum_{k=1}^{K} \frac{\mathbb{E}\Big[(I_k - \alpha_0 - \alpha_1 z_k)^2\Big]}{2\sigma_\delta^2}$$

$$+ \frac{-K}{2}\log(2\pi\sigma_w^2) - \sum_{k=1}^{K} \frac{\mathbb{E}\Big[(z_k - z_{k-1})^2\Big]}{2\sigma_w^2}.$$

E. Arousal-performance function

Using both estimated arousal and performance states, we define a relationship between the arousal state and performance state based on the Inverted-U law [24], [25].

$$Y_k = \lambda_1 X_k^2 + \lambda_2 X_k + \lambda_3 + e_k \tag{30}$$

where Y_k is a standard score of the performance state at each trial and X_k is the standard score of the average arousal that a participant has at each trial. Thus, our observed data points consist of (X,Y). e_k has been assumed to be independent and identically distributed (i.i.d.) random variable, $e_k \sim \mathcal{N}(0, \sigma_e^2)$ and, λ_1, λ_2, and λ_3 are the unknown parameters that can be estimated by robust fitting with bisquare weighting. We avoid using the ordinary least-squares method since our data points are from multiple different trials and to overcome the outlier effects, we choose robust regression analysis for estimating the coefficients. Robust fitting with bisquare weights uses an iteratively reweighted least-squares algorithm and we have used a MATLAB function *fitlm* where Y_k and X_k are the input of the function and, *purequadratic* and *RobustOpts* are the additional options that have been applied. After estimating λ_1, λ_2, and λ_3, the i.i.d. noise term e_k and its variance σ_e^2, can be calculated given the fitted model and the observed data points.

III. Results

We evaluate the outcome of the arousal and performance decoders and compare the proposed model with our estimated states based on the dataset described above. Fig. 2 shows an example of the decoded arousal state for one participant (participant 1), where the first subplot is representing the deconvolved skin conductance signal during the experiment. Applying the deconvolution algorithm, we detect neural impulses due to ANS activation during the experiment as described Fig. 1 and second sub-panel of Fig. 2. We present the probability of observing an impulse (a_j) in the fourth sub-panel of Fig. 2 which has a direct relationship with the estimated state. Similar to [16], we define a high arousal index (HAI) which can be calculated by $p(x_j > x_{\text{threshold}})$ where the threshold has been set to the median of the state values. There is a consistence difference between the calming and vexing region in terms of the observed impulse amplitude, estimated states values, and HAI.

Fig. 3 illustrates an example of the performance state estimation results for one participant. The first sub-panel shows the reaction time for each trial (black dots) and reconstructed reaction time (black curve) that has been reconstructed using equation (19) with the estimated parameters. The second sub-panel describes the responses for each trial. Similar to the arousal case, we can calculate the high performance index or HPI (fourth sub-panel). By comparing second, third, and fourth sub-panel, we observe the direct relationship between the number of correct responses, the estimated state values, and HPI which exhibits the steadiness of the estimation results. Additionally, based on the fact that 3-back tasks are more challenging than 1-back tasks, we expect to have a higher probability of obtaining correct responses during the 1-back tasks. The estimated p_k and HPI depict that our results meet this expectation.

Based on obtained arousal and performance estimate, we perform our regression analysis by fitting the proposed model in equation (30) on 704 data points which is relatively large sample size compared to the number of unknowns in the model. According to Fig. 4 where the x-axis is the standard score of the estimated arousal states during trials and y-axis stands for the standard score of the performance states, the Inverted-U law holds for all participants while the slopes are different. The estimated coefficients ($\hat{\lambda}$) in Table I, reveals that for all the participants, $\hat{\lambda}_1$ is negative which depicts the inverted attribute of the presumed quadratic nature. Moreover, we perform the hypothesis test that the corresponding coefficient is equal to zero or not. The corresponding p-values are provided in Table II. From Table II, we see that the estimated λ_1 are statistically significant for all participant with 1% significant level suggesting strong evidence of the quadratic relationship.

IV. Discussion and Conclusion

The experiment was originally designed to detect the influence of musical neurofeedback on cognitive engagement. Using a state-space modeling approach, we decode cognitive arousal and performance states. Thereafter, we

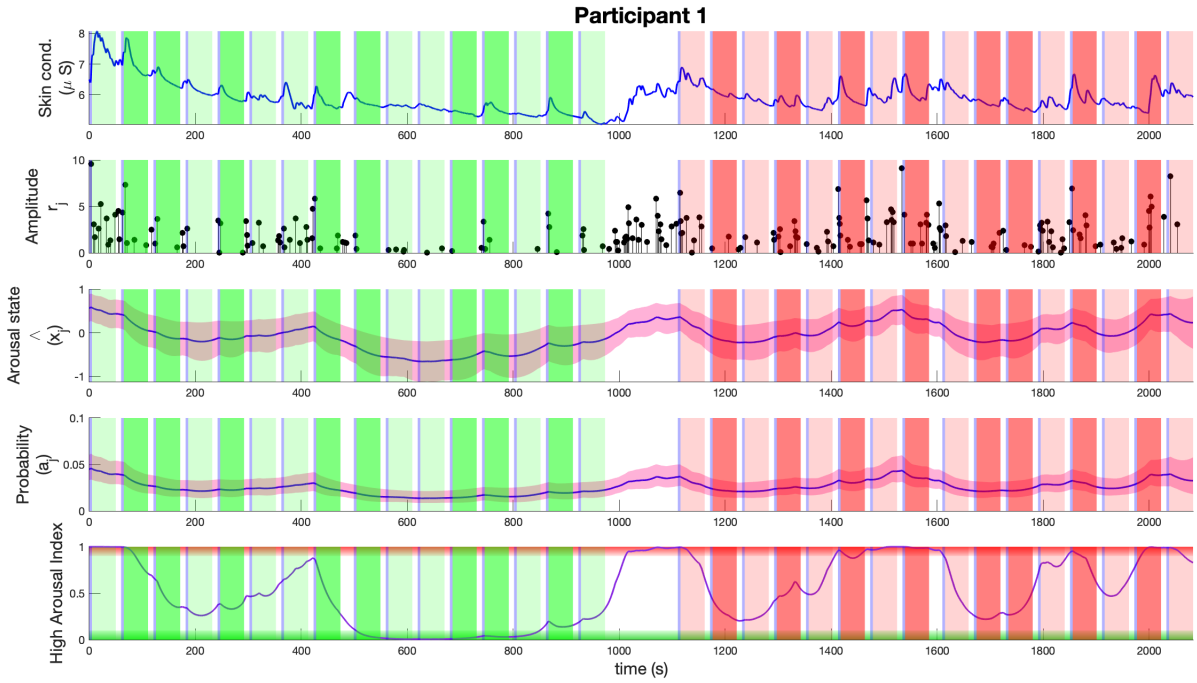

Fig. 2: **Example of arousal state estimation for a participant.** The sub-panels for the figure respectively depict: the skin conductance signal; the deconvolved neural impulses due to ANS activation; the estimated state and its 95% confidence limits; the probability of impulse occurrence and its 95% confidence limits; high arousal index or HAI. The background colors in each sub-panel depict: the 1-back task during calming session (light green); the 3-back task during calming session (dark green); the 1-back task during vexing session (light red); the 3-back task during vexing session (dark red).

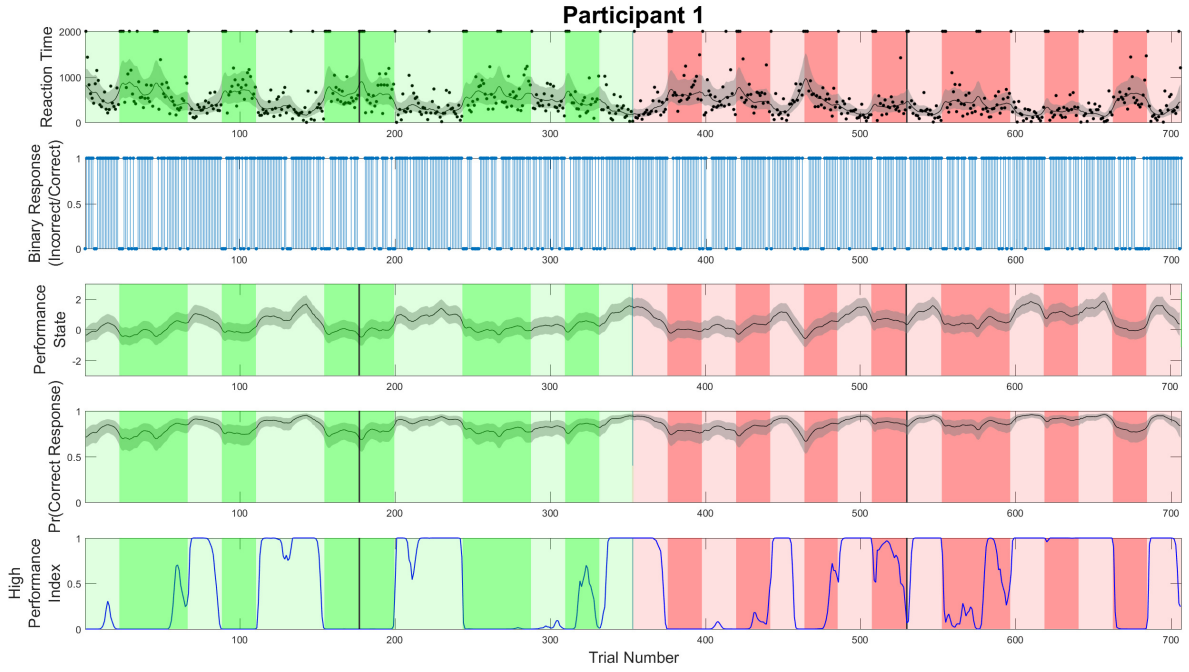

Fig. 3: **Example of performance state estimation for one Participant.** The sub-panels for the figure respectively represent: the reaction time (black dots), reconstructed reaction time (black curve) and its 95 % confidence limits; correct/incorrect response; the state estimate and its 95 % confidence limits; the probability of correct response and its 95% confidence limits; high performance index or HPI. The background colors in each sub-panel mark: the 1-back task during the calming session (light green); the 3-back task during the calming session (dark green); the 1-back task during the vexing session (light red); the 3-back task during the vexing session (dark red).

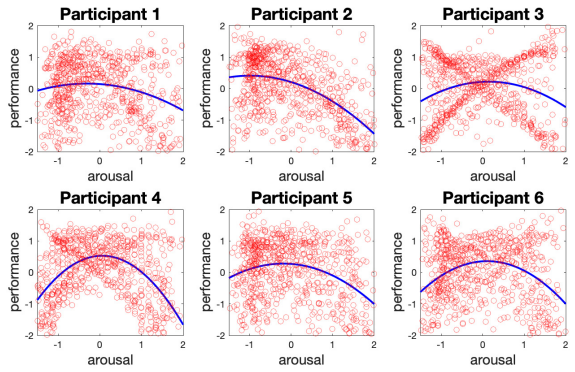

Fig. 4: **Arousal-Performance diagram** In each of the sub-panels the red circles stand for the observed data points and blue curves denote the fitted model for each of the participants.

evaluate the existence of Yerkes–Dodson law via regression analysis. According to the presented results, at the beginning of most of the task blocks, we observe some neural impulses in the inferred ANS activation which can be related to the participant's initial excitement. Right after entering the vexing session, the skin conductance signal value (first sub-pannel in Fig. 2) increases, which can intensify the music's effects on the psychological arousal of the participant.

According to the presence of the Yerkes–Dodson law or the inverted-U function in Fig. 4, our results indicate the feasibility of regulating the arousal state such that it maximizes the performance of the participant using music. Based on the fact that in this study our participants performed multiple trails of different tasks (i.e., 1-back and 3-back tasks during relaxing and vexing music blocks), each of these variations might impact each participant in a different way. This might be causing variations in the task-based noise models when linking the decoded cognitive arousal to the decoded performance states and impacting how the inverted-U relationship holds for each subject. Examining the HAI and HPI in Fig. 2 and Fig. 3, respectively, the HAI, which expresses the probability of impulse occurrence, is low during the calming session and high during the vexing session. Conversely, mean value of HPI, which has a direct relationship with the performance state value, is higher during the vexing region compared to the calming region. Consequently, we can conclude that the arousal state can be regulated by musical neurofeedback in an attempt to optimize cognitive performance.

In future, we plan to utilize multi-modal and multi-channel signals to reliably infer brain activity [31], [32] related to cognitive arousal. We then plan to utilize the inferred multi-modal brain activity to estimate the hidden brain states with multiple observations [15]. In particular, we plan to develop multiple-input and multiple-output (MIMO) models and decoders that link latent arousal and performance states to multiple types of binary and continuous physiological measures, and simultaneously decode these cognitive states by considering the Yerkes–Dodson law. We plan to consider different noise models for linking cognitive arousal to cognitive performance to better capture the inverted-U relationship between these two brain states during multiple trials based on different tasks. Finally, we plan to design a closed-loop system with non-invasive actuation such as music to maximize performance and productivity by regulating arousal [33].

TABLE I: Estimated parameters of Arousal-Performance model

Participant	$\hat{\lambda}_1$	$\hat{\lambda}_2$	$\hat{\lambda}_3$	σ_e^2
1	-0.1598	-0.0994	0.1465	0.9346
2	-0.2061	-0.4098	0.2098	0.7394
3	-0.2336	0.0651	0.2179	0.9234
4	-0.5796	0.0661	0.5281	0.7630
5	-0.2676	-0.1024	0.2714	0.8876
6	-0.3790	0.0808	0.3542	0.88578

TABLE II: Arousal-performance regression model results

	p-value		
Participant	λ_1	λ_2	λ_3
1	3.14e-05	0.0197	0.0048
2	4.13e-09	2.04e-25	5.71e-06
3	1.20e-07	0.10985	0.0001
4	5.89e-45	0.0594	8.34e-25
5	3.53e-18	0.0110	4.13e-08
6	2.91e-18	0.0455	1.7e-10

ACKNOWLEDGMENT

The authors thank Dilranjan S. Wickramasurya and Srinidhi Parshi for their help during data collection and preparing the dataset.

REFERENCES

[1] M. W. Eysenck, "Arousal, learning, and memory.," *Psychological bulletin*, vol. 83, no. 3, p. 389, 1976.

[2] M. R. Amin and R. T. Faghih, "Identification of sympathetic nervous system activation from skin conductance: A sparse decomposition approach with physiological priors," *IEEE Transactions on Biomedical Engineering*, 2020.

[3] W. K. Kirchner, "Age differences in short-term retention of rapidly changing information.," *Journal of experimental psychology*, vol. 55, no. 4, p. 352, 1958.

[4] S. Parshi, R. Amin, H. F. Azgomi, and R. T. Faghih, "Mental workload classification via hierarchical latent dictionary learning: A functional near infrared spectroscopy study," in *2019 IEEE EMBS International Conference on Biomedical & Health Informatics (BHI)*, pp. 1–4, IEEE, 2019.

[5] J. A. Lehmann and T. Seufert, "The influence of background music on learning in the light of different theoretical perspectives and the role of working memory capacity," *Frontiers in psychology*, vol. 8, p. 1902, 2017.

[6] Y. Jing, S. Jing, C. Huajian, S. Chuangang, and L. Yan, "The gender difference in distraction of background music and noise on the cognitive task performance," in *2012 8th International Conference on Natural Computation*, pp. 584–587, IEEE, 2012.

[7] M. Nithya.S, "Analysis of music effect on n-back task performance," pp. 38–42, 2016.

[8] A. C. Smith, L. M. Frank, S. Wirth, M. Yanike, D. Hu, Y. Kubota, A. M. Graybiel, W. A. Suzuki, and E. N. Brown, "Dynamic analysis of learning in behavioral experiments," *J. Neuroscience*, vol. 24, no. 2, pp. 447–461, 2004.

[9] A. C. Smith, M. R. Stefani, B. Moghaddam, and E. N. Brown, "Analysis and design of behavioral experiments to characterize population learning," *Journal of Neurophysiology*, vol. 93, no. 3, pp. 1776–1792, 2005.

[10] T. P. Coleman, M. Yanike, W. A. Suzuki, and E. N. Brown, "A mixed-filter algorithm for dynamically tracking learning from multiple behavioral and neurophysiological measures," *The dynamic brain: An exploration of neuronal variability and its functional significance*, pp. 3–28, 2011.

[11] X. Deng, R. T. Faghih, R. Barbieri, A. C. Paulk, W. F. Asaad, E. N. Brown, D. D. Dougherty, A. S. Widge, E. N. Eskandar, and U. T. Eden, "Estimating a dynamic state to relate neural spiking activity to behavioral signals during cognitive tasks," in *2015 37th Annual International Conference of the IEEE Engineering in Medicine and Biology Society (EMBC)*, pp. 7808–7813, IEEE, 2015.

[12] M. J. Prerau, A. C. Smith, U. T. Eden, Y. Kubota, M. Yanike, W. Suzuki, A. M. Graybiel, and E. N. Brown, "Characterizing learning by simultaneous analysis of continuous and binary measures of performance," *Journal of neurophysiology*, vol. 102, no. 5, pp. 3060–3072, 2009.

[13] M. M. Shanechi, R. C. Hu, M. Powers, G. W. Wornell, E. N. Brown, and Z. M. Williams, "Neural population partitioning and a concurrent brain-machine interface for sequential motor function," *Nature neuroscience*, vol. 15, no. 12, pp. 1715–1722, 2012.

[14] M. M. Shanechi, R. C. Hu, and Z. M. Williams, "A cortical–spinal prosthesis for targeted limb movement in paralysed primate avatars," *Nature communications*, vol. 5, no. 1, pp. 1–9, 2014.

[15] D. S. Wickramasuriya and R. T. Faghih, "A mixed filter algorithm for sympathetic arousal tracking from skin conductance and heart rate measurements in pavlovian fear conditioning," *PloS one*, vol. 15, no. 4, p. e0231659, 2020.

[16] D. S. Wickramasuriya and R. T. Faghih, "A marked point process filtering approach for tracking sympathetic arousal from skin conductance," *IEEE Access*, vol. 8, pp. 68499–68513, 2020.

[17] T. Yadav, M. M. U. Atique, H. F. Azgomi, J. T. Francis, and R. T. Faghih, "Emotional valence tracking and classification via state-space analysis of facial electromyography," in *2019 53rd Asilomar Conference on Signals, Systems, and Computers*, pp. 2116–2120, IEEE, 2019.

[18] M. B. Ahmadi, A. Craik, H. F. Azgomi, J. T. Francis, J. L. Contreras-Vidal, and R. T. Faghih, "Real-time seizure state tracking using two channels: A mixed-filter approach," in *2019 53rd Asilomar Conference on Signals, Systems, and Computers*, pp. 2033–2039, IEEE, 2019.

[19] D. S. Wickramasuriya and R. T. Faghih, "A bayesian filtering approach for tracking arousal from binary and continuous skin conductance features," *IEEE Transactions on Biomedical Engineering*, vol. 67, no. 6, pp. 1749–1760, 2019.

[20] D. S. Wickramasuriya and R. T. Faghih, "A cortisol-based energy decoder for investigation of fatigue in hypercortisolism," in *2019 41st Annual International Conference of the IEEE Engineering in Medicine and Biology Society (EMBC)*, pp. 11–14, IEEE, 2019.

[21] D. S. Wickramasuriya and R. T. Faghih, "A novel filter for tracking real-world cognitive stress using multi-time-scale point process observations," in *2019 41st Annual International Conference of the IEEE Engineering in Medicine and Biology Society (EMBC)*, pp. 599–602, IEEE, 2019.

[22] D. S. Wickramasuriya, M. Amin, R. T. Faghih, *et al.*, "Skin conductance as a viable alternative for closing the deep brain stimulation loop in neuropsychiatric disorders," *Frontiers in neuroscience*, vol. 13, p. 780, 2019.

[23] D. S. Wickramasuriya, C. Qi, and R. T. Faghih, "A state-space approach for detecting stress from electrodermal activity," in *2018 40th Annual International Conference of the IEEE Engineering in Medicine and Biology Society (EMBC)*, pp. 3562–3567, IEEE, 2018.

[24] R. M. Yerkes, J. D. Dodson, *et al.*, "The relation of strength of stimulus to rapidity of habit-formation," *Punishment: Issues and experiments*, pp. 27–41, 1908.

[25] R. M. Yerkes, *The dancing mouse*, vol. 1. Macmillan Company, 1907.

[26] A. B. Ünal, D. de Waard, K. Epstude, and L. Steg, "Driving with music: Effects on arousal and performance," *Transportation research part F: traffic psychology and behaviour*, vol. 21, pp. 52–65, 2013.

[27] S. Parshi, "A functional-near infrared spectroscopy investigation of mental workload," Master's thesis, University of Houston, 2020.

[28] M. R. Amin and R. T. Faghih, "Tonic and phasic decomposition of skin conductance data: A generalized-cross-validation-based block coordinate descent approach," in *2019 41st Annual International Conference of the IEEE Engineering in Medicine and Biology Society (EMBC)*, pp. 745–749, IEEE, 2019.

[29] M. R. Amin and R. T. Faghih, "Sparse deconvolution of electrodermal activity via continuous-time system identification," *IEEE Transactions on Biomedical Engineering*, vol. 66, no. 9, pp. 2585–2595, 2019.

[30] A. Greco, G. Valenza, A. Lanata, E. P. Scilingo, and L. Citi, "cvxeda: A convex optimization approach to electrodermal activity processing," *IEEE Transactions on Biomedical Engineering*, vol. 63, no. 4, pp. 797–804, 2015.

[31] M. R. Amin and R. T. Faghih, "Inferring autonomic nervous system stimulation from hand and foot skin conductance measurements," in *52th Asilomar Conference on Signals, Systems and Computers*, 2018.

[32] M. R. Amin and R. T. Faghih, "Robust inference of autonomic nervous system activation using skin conductance measurements: A multi-channel sparse system identification approach," *IEEE Access*, vol. 7, pp. 173419–173437, 2019.

[33] H. F. Azgomi, D. S. Wickramasuriya, and R. T. Faghih, "State-space modeling and fuzzy feedback control of cognitive stress," in *2019 41st Annual International Conference of the IEEE Engineering in Medicine and Biology Society (EMBC)*, pp. 6327–6330, IEEE, 2019.